Article

Discovery Medicine 2025; 37(197): 1105–1116
https://doi.org/10.24976/Discov.Med.202537197.98

Inhibiting NLRP3/Caspase-1/GSDMD-Mediated Pyroptosis: A New Role of GADD45B's Role in Hypertriglyceridemia-Induced Acute Pancreatitis

Shengang Zhou[1,2], Yingge Xu[2], Jianfeng Tu[2], Mao Zhang[1,3,*]

[1]Department of Emergency Medicine, Second Affiliated Hospital, Zhejiang University School of Medicine, 310009 Hangzhou, Zhejiang, China
[2]Emergency and Critical Care Center, Department of Emergency Medicine, Zhejiang Provincial People's Hospital (Affiliated People's Hospital), Hangzhou Medical College, 310014 Hangzhou, Zhejiang, China
[3]Institute of Emergency Medicine, Zhejiang University, 310058 Hangzhou, Zhejiang, China
*Correspondence: zmhz@hotmail.com (Mao Zhang)
Published: 9 June 2025

Background: Hypertriglyceridemia-induced acute pancreatitis (HTG-AP) is a severe form of pancreatitis, rapidly progressing to multiorgan failure. Growth arrest and DNA damage-inducible beta (GADD45B) play a crucial role in stress responses; however, its precise role in HTG-AP pathogenesis remains unknown. Therefore, this study aimed to elucidate the role of GADD45B in HTG-AP using both *in vitro* cellular and *in vivo* animal models.

Methods: AR42J cells were transfected with GADD45B si-RNA or overexpressed plasmids and induced with palmitic acid (PA) and caerulein (Cae) to establish an HTG-AP cellular model. The HTG-AP animal model was successfully developed by treating mice with P-407 and Cae, alongside adeno-associated virus (AAV)-shRNA interference. The transfection efficiency was assessed using quantitative PCR (qPCR) and Western blot analyses. Furthermore, cell viability was evaluated using the Cell Counting Kit-8 (CCK-8) assay, and cell death rate, inflammation levels, and pyroptosis were examined using Hoechst 33342/propidium iodide (PI) staining, enzyme-linked immunosorbent assay (ELISA), and transmission electron microscope (TEM). Moreover, protein expression levels of the pyroptotic pathway, nucleotide-binding and oligomerization domain (NOD)-like receptor family pyrin domain containing 3/Cysteine-dependent aspartate-specific protease 1/Gasdermin D (NLRP3/Caspase-1/GSDMD), were evaluated using Western blot analysis.

Results: The Co-IP assay confirmed the interaction between GADD45B and NLR family pyrin domain containing 3 (NLRP3). In the AR42J cell model of HTG-AP, GADD45B interference promoted cell viability, attenuated cell death, pro-inflammation, pyroptotic cytokines interleukin (IL)-6, tumor necrosis factor-α (TNF-α), IL-1β, IL-18, amylase, and intracellular vesicle counts ($p < 0.05$). Furthermore, AAV-shGADD45B treatment improved pancreatic injury, cell death, and pyroptosis in HTG-AP model mice ($p < 0.05$). Moreover, GADD45B knockdown suppressed the pyroptosis-related pathway NLRP3/Caspase-1/GSDMD protein levels ($p < 0.05$). However, GADD45B overexpression exhibited opposite effects, which was reserved by NLRP3 inhibitor MCC950 ($p < 0.05$).

Conclusions: This study revealed that GADD45B downregulation reduces pyroptosis by suppressing the NLRP3/Caspase-1/GSDMD axis in HTG-AP, underscoring GADD45B as a promising therapeutic target and enhancing its clinical application.

Keywords: HTG-AP; GADD45B; pyroptosis; inflammatory; NLRP3/Caspase-1/GSDMD

Introduction

Hypertriglyceridemia (HTG) is characterized by elevated serum triglyceride (TG) levels, representing an underlying metabolic disturbance [1]. When moderate to severe acute pancreatitis (AP) is complicated by effusion or necrosis, a variety of adverse events may occur, and cases with persistent organ failure carry a high mortality risk [2]. HTG has been recognized as an etiologic factor in AP, which is termed hypertriglyceridemia-induced acute pancreatitis (HTG-AP) [1]. HTG-AP most frequently occur in patients with high serum TG levels, accounting for approximately 5% of AP cases when TG levels exceed 1000 mg/dL [3]. Although patients may exhibit mild symptoms at onset, HTG-AP can progress rapidly to a critical state with multiorgan failure [4]. Therapeutic interventions like plasmapheresis and insulin therapy focus on rapid reduction of TG levels, attenuate pancreatic inflammation, and preserve organ function [5]. Nevertheless, the precise etiology and progression of HTG-AP remain unexplored, underscoring the need to delve into its molecular underpinnings and uncover therapeutic targets to enhance patient outcomes.

Pyroptosis is a form of programmed cell death triggered by activating pro-inflammatory inflammasomes, and exhibits features of both apoptosis and necroptosis [6,7].

This cell death mechanism is largely governed by the initiation of inflammatory responses involving proteins such as the NLR family pyrin domain containing 3 (NLRP3) and absent in melanoma 2 (AIM2), which activate caspase-1, thereby promoting the pyroptotic process. Caspase-1 activation enhances the secretion of pro-inflammatory cytokines, notably interleukin (IL)-1β and IL-18 [8]. Furthermore, pyroptosis has been linked to the pathogenesis of various clinical conditions, including cardiovascular diseases, neurodegenerative disorders, and HTG-AP [9–11]. A study by Wang *et al*. [12] revealed that baicalein can reduce cellular pyroptosis and inflammation in HTG-AP by modulating the NLRP3/Caspase-1 axis, thereby attenuating pancreatic injury. Thus, inhibiting pyroptotic cascades represents a potential therapeutic strategy for alleviating HTG-AP symptoms.

Growth arrest and DNA damage-inducible beta (GADD45B), a member of the GADD45 family, play a crucial role in stress responses [13]. It influences disease progression by regulating the cell cycle, increasing DNA repair, and modulating cellular proliferation and cell death cascades [14,15]. Studies have revealed that GADD45B is integral to myeloid cell responses to differentiation-inducing cytokines and inflammatory triggers [16] and has been found to induce apoptosis in diabetic nephropathy [17]. Moreover, elevated GADD45B levels have been linked to lipid accumulation [18]. However, its precise role in the pathogenesis of HTG-AP remains unknown.

Therefore, this study aimed to explore whether GADD45B exacerbates HTG-AP by facilitating inflammation-induced pyroptosis. The impact of GADD45B on pyroptosis was assessed utilizing both cellular and animal models of HTG-AP in this study. These findings are expected to lay a robust theoretical foundation for the therapeutic potential of GADD45B in pancreatic disease management.

Materials and Methods

Cell Culture

AR42J, a rat pancreatic exocrine cell line (iCell-r002, iCell, Shanghai, China), was seeded in F12K medium enriched with 10% fetal bovine serum (FBS) (R30423, TransGen Biotech, Beijing, China) and incubated at 37 °C with a 5% CO_2. Cells were confirmed by morphological identification and tested negative for mycoplasma.

Cell Transfection and HTG-AP Cell Model Establishment

AR42J cells were transfected with si-NC, si-GADD45B, oe-GADD45B, or oe-NC plasmid (Azenta Life Sciences, Suzhou, China) using Lipofectamine^{TM}3000 Transfection Reagent, adhering to the manufacturer's protocols (Invitrogen, Carlsbad, CA, USA). si-GADD45B primer sequences were as follows: Forward primer: 5′-CGUUCUGCUGCGACAAUGATT-3′, Reverse primer: 5′ UCAUUGUCGCAGCAGAACGTT-3′. Forty-eight hours post-transfection, the HTG-AP cell model was induced by treating them with 0.5 mmol/L of palmitic acid (PA) (B21705, Shanghai Yuanye Biotechnology Co., Ltd., Shanghai, China) and 5 nM of caerulein (Cae) (MB2573, Meilunbio, Dalian, China) [11]. After that, they were incubated with NLRP3 inhibitor MCC950 (20 nM, HY-12815, MedChemExpress, Monmouth Junction, NJ, USA) for 12 hours. Finally, the cells were categorized into two groups:

- Group 1: Control, Model, Model + si-NC, and Model + si-GADD45B.
- Group 2: Control, Model, MCC950, oe-NC oe-GADD45B, and oe-GADD45B + MCC950.

Experimental Animals

Specific pathogen-free (SPF) male C57BL/6 mice (weighed 18–22 g and aged 6–8 weeks) were procured from Shanghai SLAC Laboratory Animal Breeding Company (License No. SCXK (Hu) 2022-0004) and daily nurtured and housed by Zhejiang Eyong Pharmaceutical R&D Co., Ltd. (License No. SYXK (Zhe) 2023-0027). Ethical approval for animal experiments was obtained from the Ethics Committee of Zhejiang Eyong Pharmaceutical R&D Co., Ltd. Animal Center (Approval No. ZJEY-20230814-01).

Model Induction and Grouping

C57BL/6 mice (n = 48) were randomly allocated into six groups (n = 8 per group), including the control group, AP group, HTG group, HTG-AP group, HTG-AP + adeno-associated virus (AAV)-NC group, and HTG-AP + AAV-GADD45B group. To examine the effects of hyperlipidemia on pancreatitis, separate AP and HTG groups were included. The HTG-AP mice model development followed a previously published protocol [19]. Briefly, the HTG model was constructed by intraperitoneal injection of 0.5 g/kg of P-407 (9003-11-6, Sigma, St. Louis, MO, USA) once daily for 28 days in all groups except control and AP. Subsequently, AP was induced in all groups except control through intraperitoneal administration of Cae at a total dose of 50 µg/kg at hourly intervals for 10 times. For gene modulations, mice in the HTG+AP+AAV-shNC and HTG+AP+AAV-shGADD45B groups were injected with 5×10^{11} vector genomes of AAV-shNC or AAV-shGADD45B (Azenta Life Sciences, Suzhou, China) in the tail vein at 24, 48, and 72 hours before the first Cae dose [20]. The control group received equivalent volumes of phosphate buffer solution (PBS) following the same injection regimen. Twenty-four hours after model induction, all mice were euthanized using carbon dioxide inhalation, and blood and pancreatic tissues were harvested for further analysis.

Table 1. Primers used in qPCR.

Gene	Forward Primer (5′-3′)	Reverse Primer (5′-3′)
Rat *GADD45B*	GGCGGCCAAACTGATGAATG	TGTATGACAGTTCGTGACCAGG
Rat *β-actin*	GTCACCCACACTGTGCCCATCT	ACAGAGTACTTGCGCTCAGGAG

GADD45B, growth arrest and DNA damage-inducible beta; qPCR, quantitative PCR.

Table 2. A list of antibodies used in Western blot analysis.

Antibody	Source	Cat No.	Dilutions
GADD45B antibody	Affinity	DF2375	1:1000
NLRP3 antibody	Affinity	DF7438	1:1000
Caspase-1 antibody	Affinity	AF5418	1:1000
Cleaved caspase-1 antibody	Affinity	AF4005	1:1000
GSDMD antibody	Affinity	AF4012	1:1000
Anti-rabbit IgG, HRP-linked antibody	CST	7074	1:6000
β-actin antibody	Proteintech	81115-1-RR	1:10,000

NLRP3, NLR family pyrin domain containing 3; GSDMD, gasdermin-D; HRP, Horseradish peroxidase.

qPCR

Total RNA was isolated from AR42J cells utilizing the TRIzol reagent, and subsequently reverse-transcribed into complementary DNA (cDNA) employing a reverse transcription kit. Quantitative PCR (qPCR) was then conducted using SYBR green (11201ES08, Yeasen, Shanghai, China). The primer sequences employed for qPCR are detailed in Table 1.

Western Blot Analysis

Total protein was extracted from pancreatic tissue samples and AR42J cells using radio immunoprecipitation (RIPA) lysis buffer (P0013B, Beyotime, Shanghai, China) and quantified using a Bicinchoninic acid assay (BCA) protein assay kit (P0012, Beyotime, Shanghai, China). Following this, equivalent volumes of protein were resolved through 10% SDS-polyacrylamide gel electrophoresis (SDS-PAGE) and transferred onto polyvinylidene difluoride (PVDF) membranes (10600023, GE Healthcare Life, Little Chalfont, Buckinghamshire, UK). Membranes were sealed in 5% skimmed milk for 2 hours at room temperature and then underwent overnight incubation with primary antibody at 4 °C. After washing with PBS, the membranes were exposed to corresponding secondary antibodies for one hour at room temperature. Finally, protein bands were visualized using an enhanced chemiluminescence (ECL) detection system. Details of the antibodies utilized in Western blot analysis are presented in Table 2.

Cell Counting Kit-8 (CCK-8)

Following transfection and establishment of the HTG+AP model, AR42J cells were seeded into 96-well plates. At 24, 48, and 72 hours, 10 µL of CCK-8 solution (C0039, Beyotime, Shanghai, China) was added to each well and incubated for one hour at 37 °C. Absorbance was then recorded at 450 nm using a microplate spectrophotometer (CMaxPlus, MD, Sunnyvale, CA, USA). Cell viability was assessed as follows: Cell viability % = (A450nm of each administered group – blank group means A450nm) / (control group means A450nm – blank group means A450nm).

Enzyme-Linked Immunosorbent Assay (ELISA)

Cell culture supernatants and mouse serum were collected by centrifugation at 4000 rpm for 20 minutes. After this, levels of IL-6 (RX203049M for mouse, RX302856R for rat), IL-1β (RX203063M for mouse, RX302869R for rat), IL-18 (RX203064M for mouse, RX302871R for rat), tumor necrosis factor-α (TNF-α) (RX202412M for mouse, RX302058R for rat), and amylase (RX200929M for mouse, RX300227R for rat) were determined using corresponding ELISA kit (Quanzhou Ruixin Biotechnology Co., Ltd., Quanzhou, China), following the manufacturer' protocols.

Hoechst 33342/Propidium Iodide (PI) Staining Assay

Cell membrane integrity was assessed using Hoechst/PI staining. AR42J cells seeded in 12-well plates and harvested mice pancreatic tissues were stained with 500 µL of Hoechst (C1025, Beyotime, Shanghai, China) and PI (S19136, Shanghai Yuanye Biotechnology Co., Ltd., Shanghai, China) solutions for 30 minutes at 4 °C in the dark, following the manufacturer's instructions. After staining, samples were rinsed with PBS and examined under a fluorescence microscope (Ts2-FC, Nikon, Japan).

Transmission Electron Microscope (TEM)

AR42J cells and pancreatic tissues were fixed in 2.5% glutaraldehyde, dehydrated, permeabilized, and embedded. Ultrathin sections of 70 nm were then prepared and stained

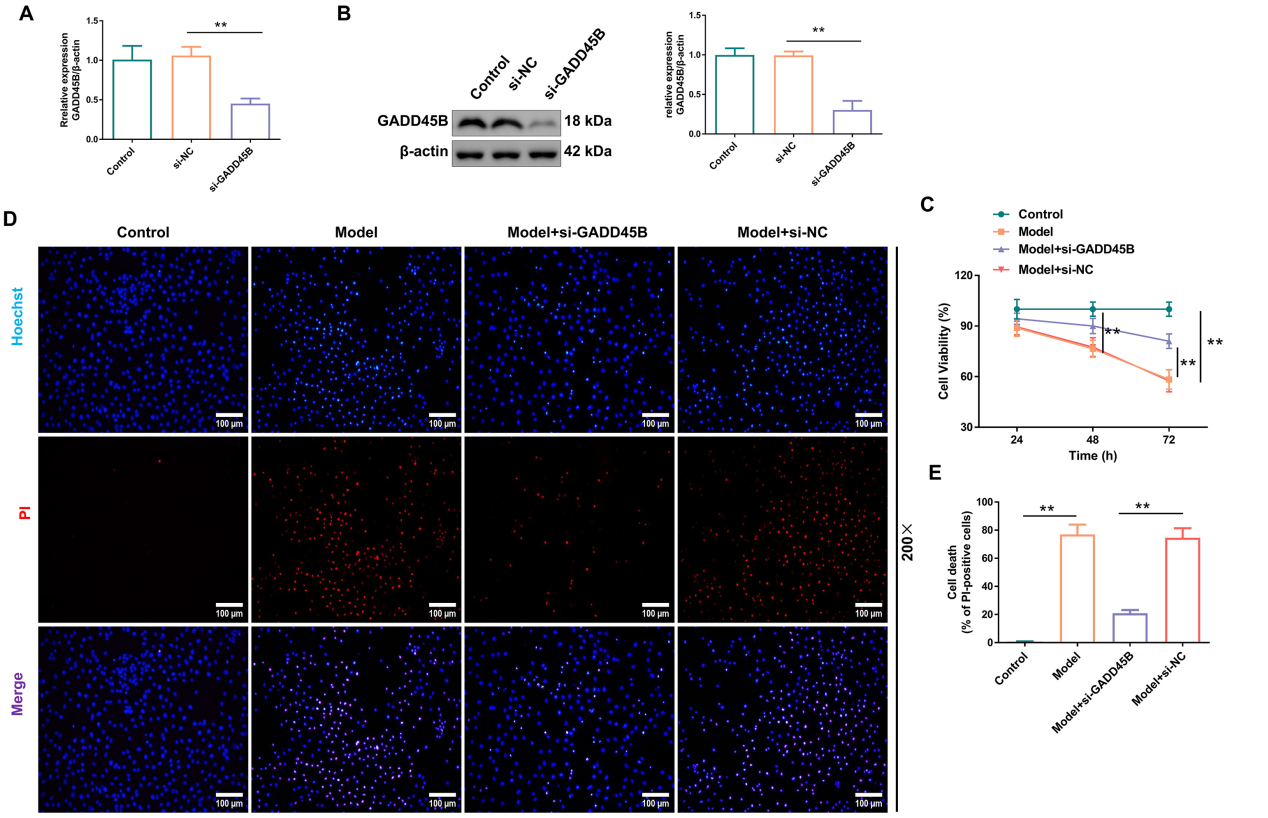

Fig. 1. GADD45B interference attenuated AR42J cell death. (A) AR42J cells were transfected with si-GADD45B or si-NC. Then, 0.5 mmol/L palmitic acid and 5 nM caerulein were added to induce the HTG-AP cell model. qPCR was employed to assess the efficiency of *GADD45B* siRNA transfection; $n = 3$. (B) The transfection efficiency of GADD45B siRNA was evaluated using Western blot analysis; $n = 3$. (C) The CCK-8 assay was used to assess cell viability at 24, 48, and 72 hours after si-GADD45B transfection; $n = 3$. (D,E) Hoechst/PI staining assay detected cell membrane damage; ×200, 100 μm; $n = 3$. AP, acute pancreatitis; $^{**}p < 0.01$. GADD45B, growth arrest and DNA damage-inducible beta; HTG, hypertriglyceridemia; HTG-AP, hypertriglyceridemia-induced acute pancreatitis; PI, propidium iodide; qPCR, quantitative PCR; CCK-8, Cell Counting Kit-8.

with 100 μL of 50% ethanol-saturated hydrogen peroxide acetate solution, and 100 μL of lead citrate for 15 min. Finally, the samples were visualized by TEM (H-7650, Hitachi, Japan).

Hematoxylin & Eosin (HE) Staining

Mouse pancreatic tissues were first fixed in a 4% paraformaldehyde and then sequentially dehydrated, cleared, and embedded in paraffin. Thin sections of approximately 4 μm thickness were prepared and subsequently immersed in hematoxylin (H3136, Sigma, St. Louis, MO, USA) for 3 minutes, thoroughly washed, and counterstained with eosin (E4009, Sigma, St. Louis, MO, USA) for 5 minutes. After final washing and clearing, sections were blocked with a neutral resin and examined under a microscope. Pathologic changes, including inflammatory cell infiltration, pancreatic cell necrosis, and edema, were scored following previously proposed criteria [21].

Immunofluorescence Staining

Mouse pancreatic tissues were initially fixed in 4% paraformaldehyde, embedded, and cryosections of 4 μm thickness were prepared. Sections were baked and dehydrated at 62 °C, followed by deparaffinization, and subjected to antigen retrieval and permeabilization. The sections were then incubated overnight at 4 °C with GSDMD antibody (AF4012, Affinity, Melbourne, Australia, dilutions: 1:100). On the following day, sections were washed with PBS and incubated with a secondary antibody at room temperature for one hour. Nuclei were stained with 2-(4-Amidinophenyl)-6-indolecarbamidine dihydrochloride (DAPI) (ab104139, Abcam, Cambridge, MA, USA), and the sections were mounted. Finally, tissue sections were examined under a fluorescence microscope, and representative images were recorded.

Co-Immunoprecipitation (CO-IP)

Cells were washed with PBS and then lysed for 20 minutes in a pre-cooled lysis solution. Cell lysates were

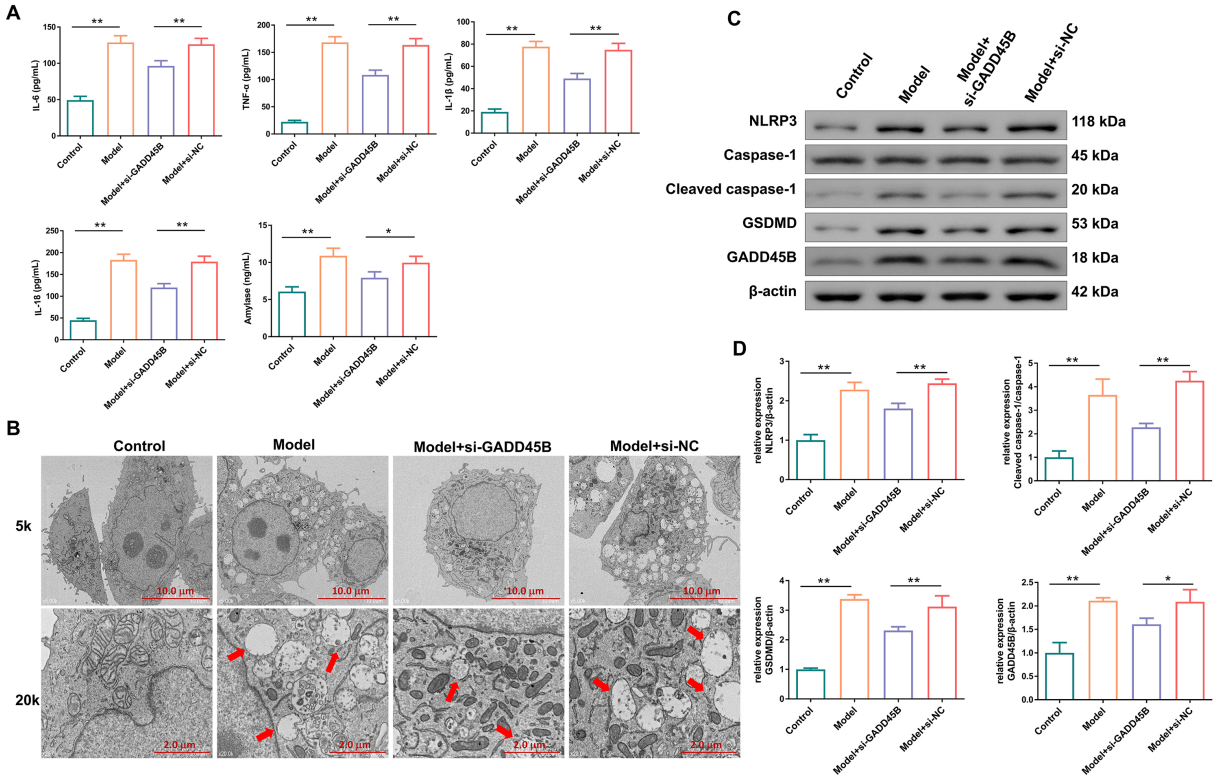

Fig. 2. The effect of si-GADD45B on inflammation and pyroptosis in the HTG-AP cell model. (A) ELISA was employed to evaluate interleukin (IL)-6, tumor necrosis factor-α (TNF-α), IL-1β, IL-18, and amylase levels in the cells supernatants; $n = 6$. (B) TEM was conducted to examine alterations in cellular ultrastructure; $\times$5 k, 10 µm; $\times$20 k, 2 µm; red arrows indicate intracellular vesicles. (C,D) Western blot analysis was used to quantify pyroptosis-related protein expression levels, including NLRP3, caspase-1, cleaved caspase-1, GSDMD, and GADD45B; $n = 3$. *$p < 0.05$, **$p < 0.01$. ELISA, Enzyme-Linked Immunosorbent Assay; TEM, transmission electron microscopy.

centrifuged, and the supernatant was pass through a 0.22 µm membrane filter. The filtrate was incubated with IgG beads for 3 hours to remove impurities, then centrifuged, and a portion of supernatant was reserved as the input control sample (mixed with 2$\times$ loading buffer). The remaining lysate was incubated overnight with Protein A agarose beads at 4 °C. Beads were washed and then incubated with anti-Flag-tag and anti-c-Myc antibodies for one hour at room temperature. Following a final wash with PBS, immune complexes were eluted with 1$\times$ loading buffer and boiled for 5 minutes. Samples were then stored at –20 °C until Western blot analysis.

Statistical Analysis

Data were analyzed using SPSS 20.0 software (IBM Corporation, Armonk, NY, USA). Continuous variables were expressed as mean $\pm$ standard deviation (SD). For normally distributed data, group comparisons were conducted using one-way analysis of variance (ANOVA) with Dunnett's T3 post hoc test. However, non-normal distributed data was assessed using the Kruskal-Wallis H test. A p-value of <0.05 was considered statistically meaningful.

Results

GADD45B Interference Attenuated Cell Death of HTG-AP Stimulated AR42J Cells

AR42J cells were transfected with si-NC or si-GADD45B, and transfection efficiency was confirmed using qPCR and Western blot analysis (Fig. 1A,B). CCK-8 results revealed that the model group showed a significant reduction in cell viability at 48 and 72 hours compared to the control group ($p < 0.01$). However, si-GADD45B treatment substantially elevated cell viability at 72 hours compared to the model + si-NC group ($p < 0.01$, Fig. 1C). After HTG-AP induction using PA and Cae, Hoechst/PI staining revealed a significantly higher cell death rate in the model group ($p < 0.01$, Fig. 1D,E), an effect that was mitigated by si-GADD45B ($p < 0.01$).

si-GADD45B Inhibited Inflammation and Pyroptosis in HTG-AP Cell Model

Increased serum amylase is an indicator of HTG-AP [22]. In this study, we assessed inflammation and pyroptosis cytokines alongside amylase using ELISA (Fig. 2A). The levels of IL-6, TNF-α, IL-1β, IL-18, and amylases

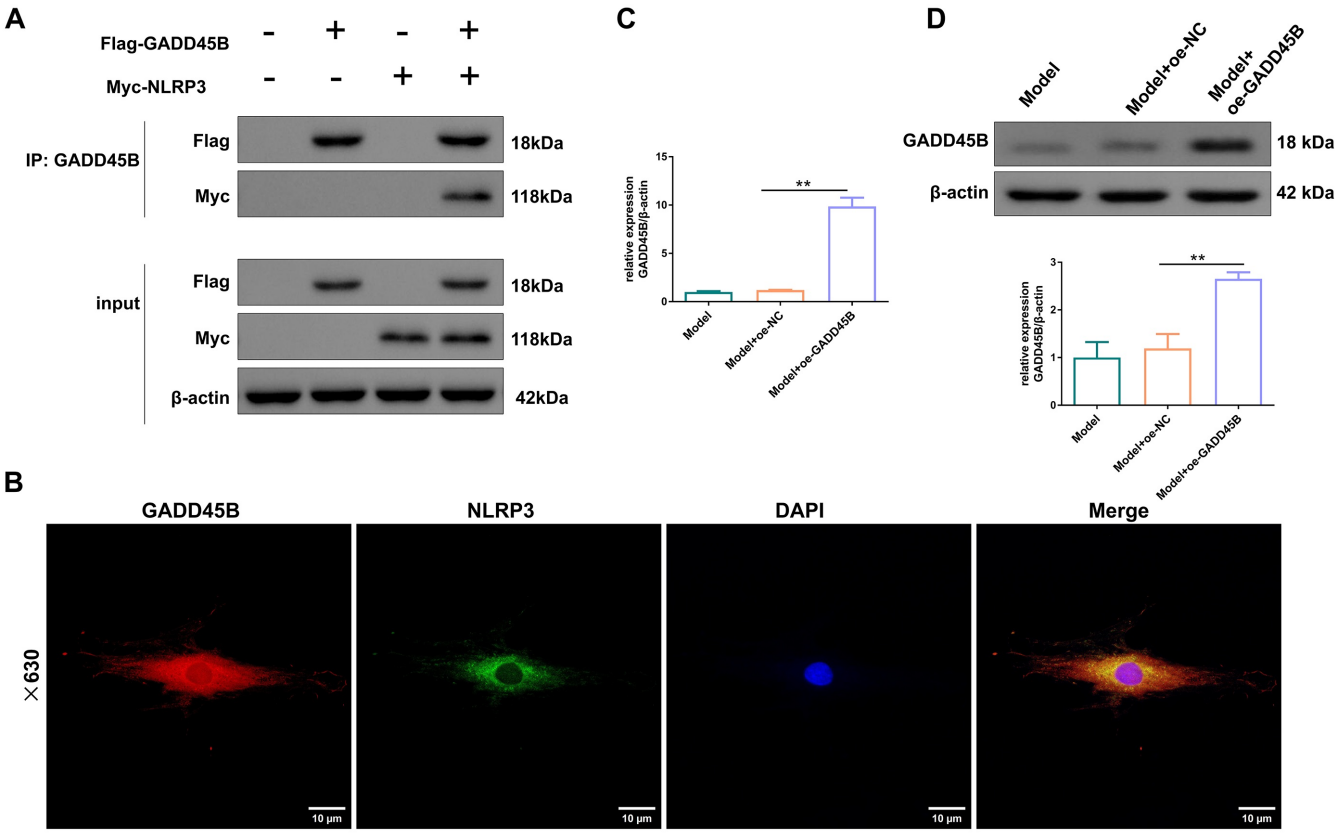

Fig. 3. Interaction between GADD45B and NLRP3 and construction of GADD45B overexpression cell lines. (A) Co-IP of Flag-GADD45B with Myc-NLRP3 from HEK293T cells. (B) Immunofluorescence detection of GADD45B co-localization with NLRP3; ×630, 10 μm. (C) qPCR revealed the transfection efficiency of GADD45B in AR42J cells. (D) Western blot analysis demonstrated the transfection efficiency of GADD45B in AR42J cells. $^{**}p < 0.01$.

were substantially higher in the model group than those in the control group ($p < 0.01$), which were significantly reduced after si-GADD45B treatment ($p < 0.05$ or $p < 0.01$). As pyroptosis leads to cell membrane rupture [23], TEM was applied to evaluate structural alterations (Fig. 2B). Control cells demonstrated intact membranes without intracellular vesicles, whereas model and model + si-NC cells displayed abundant vesicle formation and membrane disruption. However, si-GADD45B treatment significantly reduced intracellular vesicle formation and promoted membrane integrity. Furthermore, Western blot analysis showed that si-GADD45B treatment substantially suppressed the expression of NLRP3, cleaved caspase-1, gasdermin-D (GSDMD), and GADD45B in the HTG-AP cell model ($p < 0.05$ or $p < 0.01$, Fig. 2C,D).

GADD45B Overexpression Promoted Pyroptosis by Activating NLRP3 in the HTG-AP Cell Model

The Co-IP assay confirmed the interaction between GADD45B and NLRP3 (Fig. 3A), and the immunofluorescence co-localization assay showed their co-localization within the cytoplasm (Fig. 3B). In AR42J cells, the transfection efficiency of oe-NC and oe-GADD45B were confirmed using qPCR and Western blot analysis, indicating substantially increased GADD45B levels ($p < 0.01$, Fig. 3C,D).

CCK-8 assay showed that AR42J cell viability was significantly reduced in the model group than in the control group ($p < 0.01$), and viability was restored after MCC950 treatment ($p < 0.05$ or $p < 0.01$). In contrast, GADD45B overexpression further inhibited viability ($p < 0.05$ or $p < 0.01$), an effect reversed after MCC950 addition ($p < 0.05$ or $p < 0.01$, Fig. 4A). Furthermore, GADD45B overexpression significantly elevated the levels of inflammatory markers (IL-6, TNF-α, IL-1β, and IL-18) and amylase ($p < 0.05$ or $p < 0.01$), which were inhibited by MCC950 (Fig. 4B). TEM analysis showed a significant increase in intracellular vesicles in the model group ($p < 0.01$), which were reduced by MCC950 ($p < 0.05$) and further augmented by GADD45B overexpression ($p < 0.01$) (Fig. 4C). However, the impact of oe-GADD45B on the pyroptotic body was offset by NLRP3 inhibition. Western blot analysis confirmed that MCC950 suppressed NLRP3 pathway protein expression levels ($p < 0.05$ or $p < 0.01$), whereas GADD45B overexpression activated this pathway, which could be blocked by MCC950 (Fig. 4D).

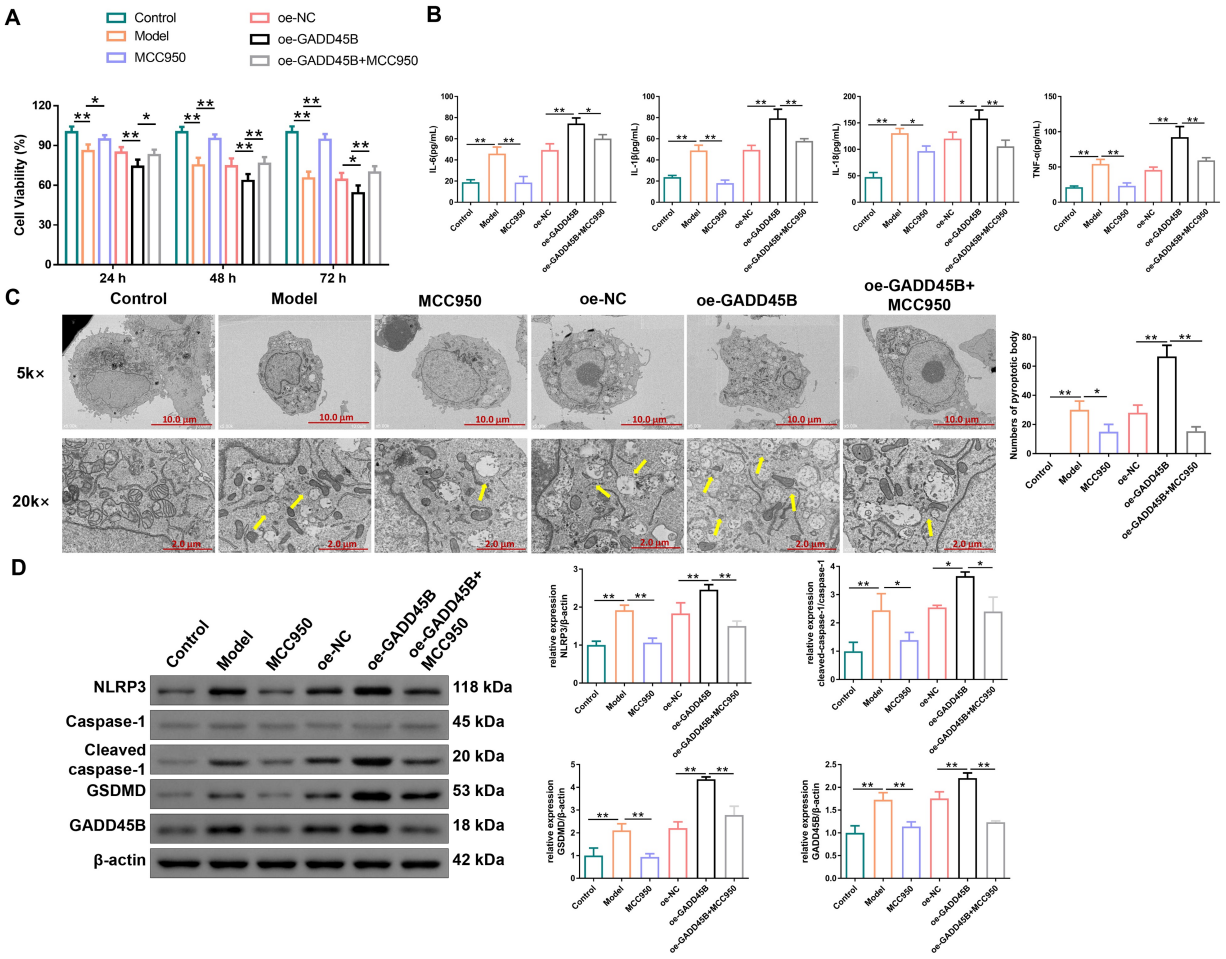

Fig. 4. GADD45B overexpression promoted pyroptosis by activating NLRP3 in the HTG-AP cell model. (A) The CCK-8 was used to assess cell viability at 24, 48, and 72 hours; n = 6. (B) The levels of IL-6, IL-1β, IL-18, TNF-α, and amylase were determined using ELISA; n = 6. (C) The numbers of pyroptosome were observed using TEM; ×5 k, 10 µm; ×20 k, 2 µm; yellow arrows indicate pyroptosome. (D) Western blot analysis indicated protein expression levels of NLRP3, caspase-1, cleaved caspase-1, GSDMD, and GADD45B; n = 3. *$p < 0.05$, **$p < 0.01$.

AAV-shGADD45B Transfection Improved Pancreatic Tissue Injury in HTG-AP Mice Model

In the P-407 and Cae-induced HTG-AP mice models, the successful knockdown of GADD45B by AAV-shGADD45B was confirmed (Fig. 5A). HE staining revealed intact pancreatic tissue in control mice without significant lesions, whereas the HTG group showed mild pancreatic injury. Conversely, the AP, HTG-AP, and HTG-AP+AAV-shNC groups exhibited severe pancreatic tissue edema, cellular necrosis, and a substantial inflammatory cell influx (Fig. 5B). However, AAV-shGADD45B treatment significantly alleviated these damages, reducing both necrosis and inflammatory cell infiltration. Furthermore, Hoechst/PI staining indicated increased cell death rates in the AP and HTG-AP groups compared to the control group (Fig. 5C,D), which was substantially decreased after the introduction of AAV-shGADD45B compared to the HTG+AP+AAV-shNC group.

Introduction of AAV-shGADD45B Reduced Inflammation and Pyroptosis in HTG-AP Mice Model

Serum levels of cytokines associated with inflammation and pyroptosis, as well as amylase, were assessed using ELISA (Fig. 6A). Relative to the control group, the AP, HTG, and HTG-AP groups exhibited substantially higher levels of IL-6, TNF-α, IL-1β, and IL-18 ($p < 0.01$), and the AP and HTG-AP groups also had increased amylase levels ($p < 0.01$). However, AAV-shGADD45B treatment significantly reduced these markers in the HTG-AP mice model ($p < 0.01$).

TEM showed distinct ultrastructural variations in mice pancreatic tissue (Fig. 6B). We observed that cellular morphology was preserved in control mice. In the AP group, mitochondrial cristae were indistinct or absent, whereas the HTG group displayed pronounced lipid droplets. The HTG-AP and HTG-AP+AAV-shNC groups had nearly unrecognizable mitochondria, distended endoplasmic reticulum,

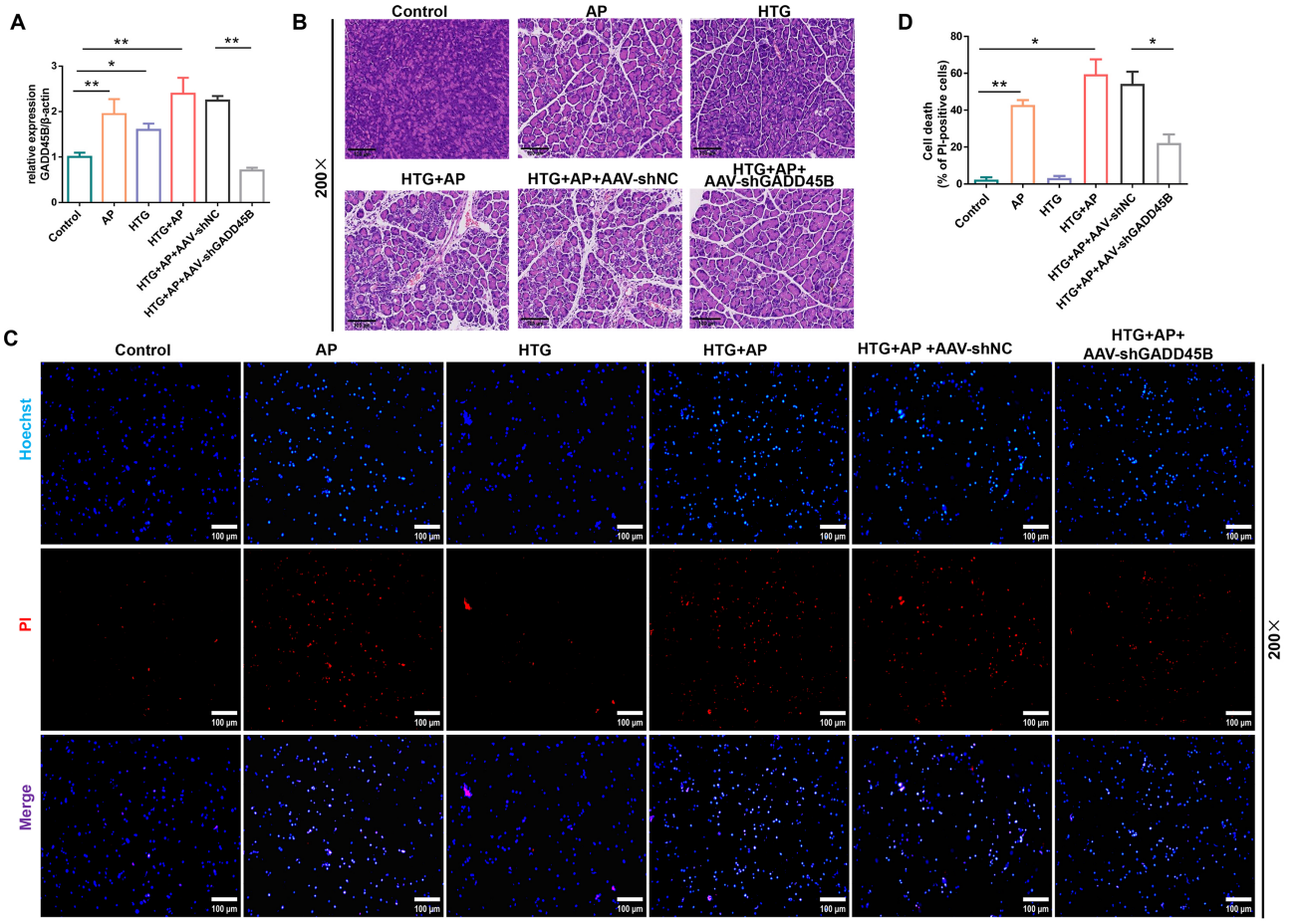

Fig. 5. Pathological changes in pancreatic tissue among HTG-AP mice model. In the P-407 and Cae-induced HTG-AP mice models, AAV-shNC and AAV-shGADD45B were injected via the tail vein before modeling, respectively. (A) The transfection efficiency of AAV-shGADD45B was assessed using a qPCR assay. n = 3. (B) HE staining revealed the histopathological alterations in mice pancreatic tissues; ×200, 100 μm. (C) Hoechst/PI staining assay detected pancreatic tissue damage in mice; ×200, 100 μm. (D) Original statistical bar graph of Hoechst/PI staining. $n = 3$. *$p < 0.05$, **$p < 0.01$. AP, acute pancreatitis; Cae, caerulein; PI, propidium iodide; AAV, adeno-associated virus; HE, Hematoxylin & Eosin.

and abundant lipid droplets. Notably, AAV-shGADD45B treatment significantly restored normal cellular architecture in HTG-AP mice.

Immunofluorescence staining showed that GSDMD expression was substantially elevated in the pancreatic tissues of AP and HTG-AP mice ($p < 0.01$), and this increase was effectively alleviated by AAV-shGADD45B ($p < 0.01$, Fig. 7A,B). Furthermore, NLRP3, caspase-1, cleaved caspase-1, GSDMD, and GADD45B levels were significantly higher in the AP, HTG, and HTG-AP groups compared to control group (Fig. 7C,D). However, the expression levels of these proteins were markedly declined after AAV-shGADD45B treatment.

Discussion

Severe HTG affects approximately 1.7% of adults, with an estimated 15–20% risk of developing HTG-AP [24]. Current therapeutic options for HTG-AP remain limited [5]. This study delved into the role of GADD45B in HTG-AP in both cellular and mice models. Our findings preliminarily uncovered that GADD45B knockdown, via si-RNA *in vitro* or AAV-shRNA *in vivo*, suppressed cell death, inflammation, and pyroptosis, mitigating HTG-AP pathology.

Triglycerides (TG) are metabolized into free fatty acids (FFAs) within the pancreas, exerting a direct cytotoxic impact on pancreatic cells [25]. Concurrently, increased lipid levels disrupt pancreatic microcirculation and trigger systemic inflammatory reactions, further aggravating pancreatic lesions [25]. Furthermore, the release of FFAs not only contributes to AP progression but is also inked to disease severity [26]. Clinically, AP is manifested by pancreatic tissue edema, acinar cell necrosis, hemorrhage, fat necrosis, and inflammatory infiltration [27]. Meng *et al.* [28] observed edema and inflammatory cell infiltration in both AP and HTG+AP rats. Similarly, our patholog-

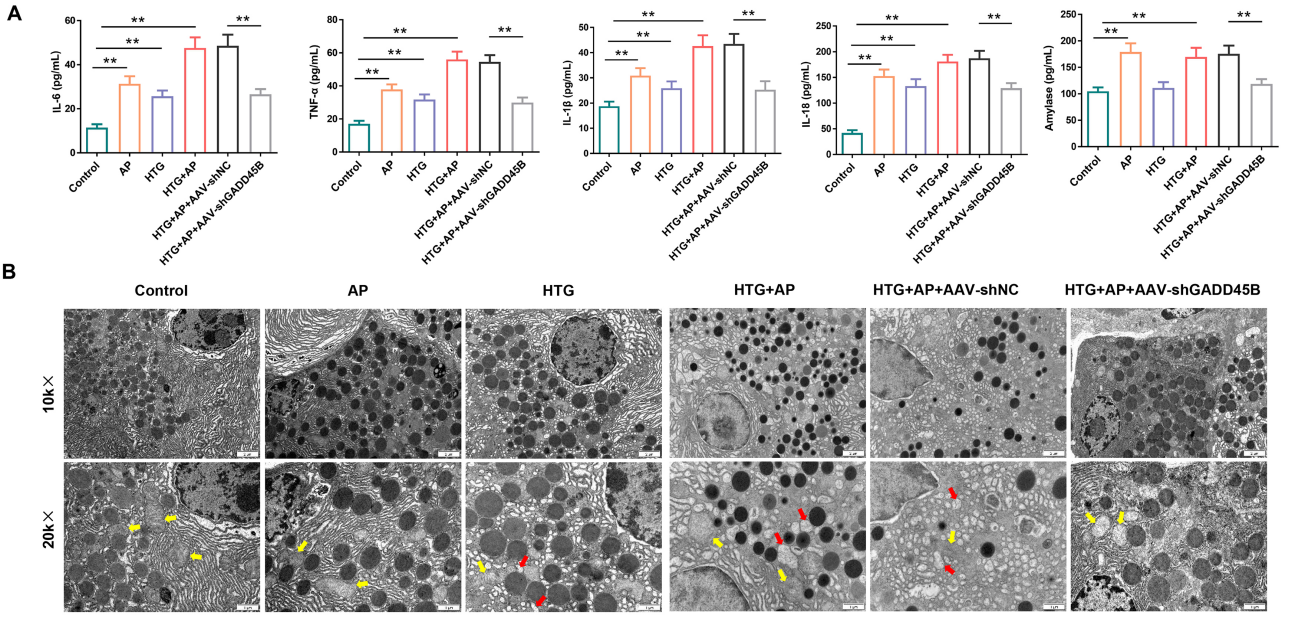

Fig. 6. The effect of GADD45B on inflammation and pyroptosis in the HTG-AP mice model. (A) Serum IL-6, TNF-α, IL-1β, IL-18, and amylase levels were determined using ELISA; $n = 6$. (B) TEM was employed to examine the ultrastructural alterations in the pancreatic tissues; $\times$10 k, 2 µm; $\times$20 k: 1 µm; red arrows indicate lipid droplets; yellow arrows represent mitochondria. $^{**}p < 0.01$.

ical scoring showed significant elevations in the AP and HTG+AP groups, confirming that HTG exacerbates pancreatic damage in AP.

Pyroptosis is a form of inflammatory cell death that triggers both local and systemic immune responses by releasing cytokines and summoning immune cells [29]. Key molecular indicators of pyroptosis include NLRP3 activation, caspase-1 cleavage, and GSDMD expression [30]. Furthermore, the stimulation of NLRP3 inflammasome triggers pro-inflammatory cytokine release, such as IL-18 and IL-1β [31]. Inhibition of NLRP3, cleaved caspase-1, GSDMD-FL, GSDMD-N, IL-1β, and IL-18 has been reported to attenuate pyroptosis and inflammation in HTG-AP [12]. Similarly, modulating the NLRP3/Caspase-1/GSDMD pathway can protect against intestinal damage in severe AP [32], and FFAs can intensify inflammation through the NLRP3-caspase1 pathway in these settings [27]. Morphologically, pyroptosis is characterized by cell swelling and membrane rupture [33]. Consistent with these observations, our HTG-AP cellular and mice models showed significant elevations in IL-6, TNF-α, IL-1β, and IL-18 levels, along with increased cell death rates. Furthermore, NLRP3, cleaved caspase-1, and GSDMD levels were significantly upregulated in both cellular and animal HTG-AP models. TEM further revealed a notable increase in intracellular vesicles and membrane rupture, all of which were reversed by the NLRP3 inhibitor MCC950. These results validate the crucial role of the NLRP3/Caspase-1/GSDMD pathways in regulating during HTG-AP.

Furthermore, this study confirmed the interaction between GADD45B and NLRP3 via Co-IP experiments. Functional assays using GADD45B knockdown and overexpression demonstrated that GADD45B regulates NLRP3/Caspase-1/GSDMD pathways. Although few studies report a direct link between GADD45B and NLRP3, existing evidence indicates indirect regulatory mechanisms. For example, GADD45B can impact Reactive Oxygen Species (ROS) levels or nuclear factor-κB (NF-κB) signaling, and it regulates the p38/JNK axis, with p38 known to phosphorylate and activate NLRP3 [34,35]. These findings indirectly corroborate our findings. Additionally, cellular experiments did not reveal significant changes in total caspase-1 protein levels, possibly due to the short stimulation period being insufficient to activate caspase-1. In contrast, in animal models, prolonged hyperlipidemia and pancreatic injury over several days may accumulate sufficient damage-associated molecular patterns (DAMPs) that promote persistent caspase-1 activation, accounting for the intergroup difference found [36].

Aberrant GADD45B expression has been observed in the pathogenesis and is known to contribute to both inflammation and cell death [37–39]. GADD45B expression is triggered by inflammatory cytokines, including IL-6, IL-12, IL-18, and TNF-α [16], and upregulation of GADD45B has been found to enhance IL-1β, IL-8, and TNF-α levels [40]. Furthermore, a study by Lu [41] revealed that IL-18 drives GADD45B expression. In the present study, IL-6, TNF-α, IL-1β, and IL-18 levels declined, and NLRP3, cleaved caspase-1, and GSDMD expression were repressed after si-GADD45B or AAV-shGADD45B intervention. Moreover, cell death was inhibited *in vitro* after GADD45B was interfered with by either si-RNA or AAV-shRNA, and pancreatic

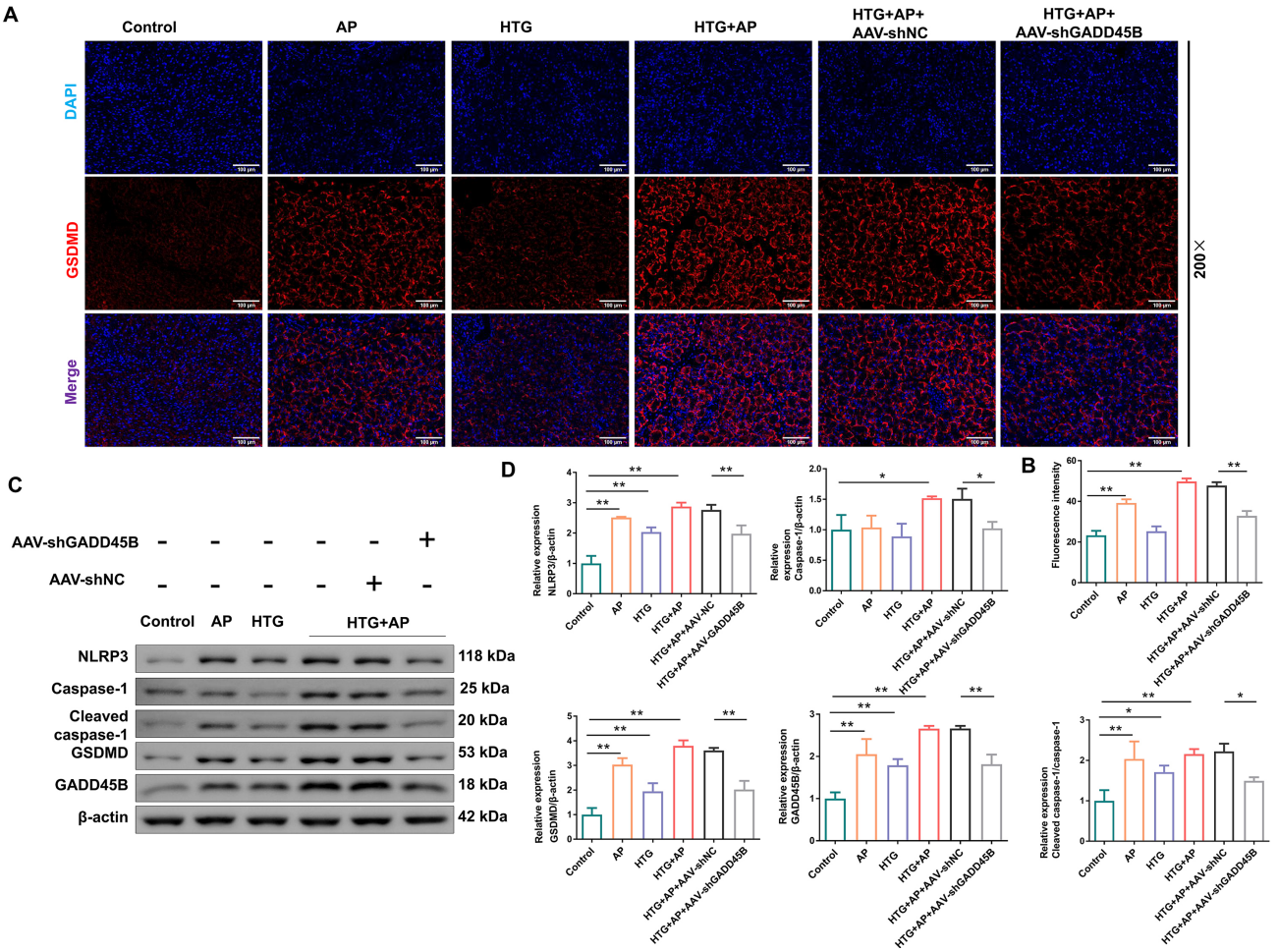

Fig. 7. The effects of GADD45B on pyroptosis-related proteins in the HTG-AP mice model. (A,B) Immunofluorescence staining detected the expression of GSDMD in mice pancreatic tissue; ×200, 100 μm; $n = 3$. (C,D) Western blot analysis was used to assess the expression levels of pyroptosis-related proteins, including NLRP3, caspase-1, cleaved caspase-1, GSDMD, and GADD45B in mice pancreatic tissues; $n = 3$. *$p < 0.05$, **$p < 0.01$.

histopathology ameliorated *in vivo*. Importantly, NLRP3 inhibitor MCC950 offset the pro-pyroptotic effect of oe-GADD45B in HTG-AP cells, suggesting that GADD45D down-regulation inhibits cellular pyroptosis and improves HTG-AP pathology.

Despite providing preliminary insights into the role of GADD45B in HTG-AP, we acknowledge several limitations in this study. First, although separate AP and HTG groups were included in *in vivo* experiments, future study should apply more robust study designs to elucidate their individual and combined impacts. Second, this study mainly relied on *in vitro* cell culture and animal models, which may not fully capture the complexities of human diseases or their pathological spectrum. Therefore, future studies should explore GADD45B's mechanisms in HTG+AP and its clinical significance by analyzing patient samples and validating in additional AP models. Furthermore, the present study suggests that GADD45B downregulation provides a novel therapeutic perspective for HTG-AP. However, this viable therapy presents multiple challenges: identifying approaches for specific GADD45B targeting, optimizing delivery systems, adjusting dosing schedules, and establishing therapeutic windows; developing reversible modulation tools, such as small-molecule inhibitors or inducible knockout systems, alongside existing therapies, and assessing possible adverse effects and safety profiles, will be crucial for future clinical utility.

Conclusions

In conclusion, down-regulation of GADD45B significantly reduced cell death, cytokine release, and pyroptosis while attenuating pathological changes in pancreatic tissues in both HTG-AP cells and mice models. These beneficial effects were driven by the inhibition of the NLRP3/Caspase-1/GSDMD pathway, preventing pyroptotic injury. These findings not only underscore GADD45B as a novel therapeutic target in HTG-AP but also provide a foundation for future investigations to further elucidate its mechanism and develop targeted treatments.

Availability of Data and Materials

The datasets generated during the current study are available from the corresponding author on reasonable request.

Author Contributions

SZ: Conceptualization, Formal analysis, Funding acquisition, Investigation, Project administration, Writing-original draft, Writing-review & editing. YX: Data curation, Formal analysis, Investigation, Methodology, Visualization. JT: Data curation, Investigation, Validation, Visualization. MZ: Conceptualization, Methodology, Project administration, Supervision, Writing-review & editing. All authors have been involved in revising it critically for important intellectual content. All authors read and approved the final manuscript. All authors have participated sufficiently in the work and agreed to be accountable for all aspects of the work.

Ethics Approval and Consent to Participate

Animal experiments were approved by the Ethics Committee of Zhejiang Eyong Pharmaceutical R&D Co., Ltd. Animal Center (No. ZJEY-20230814-01), and in accordance with the NIH guideline.

Acknowledgment

Not applicable.

Funding

This work was supported by the Foundation of Zhejiang Provincial Administration of Traditional Chinese Medicine [grant number 2019ZA015].

Conflict of Interest

The authors declare no conflict of interest.

References

[1] Kiss L, Fűr G, Pisipati S, Rajalingamgari P, Ewald N, Singh V, *et al*. Mechanisms linking hypertriglyceridemia to acute pancreatitis. Acta Physiologica (Oxford, England). 2023; 237: e13916. https://doi.org/10.1111/apha.13916.

[2] Szatmary P, Grammatikopoulos T, Cai W, Huang W, Mukherjee R, Halloran C, *et al*. Acute Pancreatitis: Diagnosis and Treatment. Drugs. 2022; 82: 1251–1276. https://doi.org/10.1007/s40265-022-01766-4.

[3] Yang AL, McNabb-Baltar J. Hypertriglyceridemia and acute pancreatitis. Pancreatology. 2020; 20: 795–800. https://doi.org/10.1016/j.pan.2020.06.005.

[4] Hu YQ, Tao X, Wu HB, Li WG, Chen DY, Liu YF, *et al*. Predicting Severity in Hypertriglyceridemia-Induced Acute Pancreatitis: The Role of Neutrophils, Calcium, and Apolipoproteins. Medical Science Monitor: International Medical Journal of Experimental and Clinical Research. 2024; 30: e942832. https://doi.org/10.12659/MSM.942832.

[5] Shafiq S, Patil M, Gowda V, Devarbhavi H. Hypertriglyceridemia-Induced Acute Pancreatitis - Course, Outcome, and Comparison with Non-Hypertriglyceridemia Associated Pancreatitis. Indian Journal of Endocrinology and Metabolism. 2022; 26: 459–464. https://doi.org/10.4103/ijem.ijem_206_22.

[6] Ketelut-Carneiro N, Fitzgerald KA. Apoptosis, Pyroptosis, and Necroptosis-Oh My! The Many Ways a Cell Can Die. Journal of Molecular Biology. 2022; 434: 167378. https://doi.org/10.1016/j.jmb.2021.167378.

[7] Wang K, Tang Z, Liu S, Liu Y, Zhang H, Zhan H. Puerarin protects renal ischemia-reperfusion injury in rats through NLRP3/Caspase-1/GSDMD pathway. Acta Cirurgica Brasileira. 2023; 38: e387323. https://doi.org/10.1590/acb387323.

[8] He Y, Hara H, Núñez G. Mechanism and Regulation of NLRP3 Inflammasome Activation. Trends in Biochemical Sciences. 2016; 41: 1012–1021. https://doi.org/10.1016/j.tibs.2016.09.002.

[9] Yarovinsky TO, Su M, Chen C, Xiang Y, Tang WH, Hwa J. Pyroptosis in cardiovascular diseases: Pumping gasdermin on the fire. Seminars in Immunology. 2023; 69: 101809. https://doi.org/10.1016/j.smim.2023.101809.

[10] Zhou J, Qiu J, Song Y, Liang T, Liu S, Ren C, *et al*. Pyroptosis and degenerative diseases of the elderly. Cell Death & Disease. 2023; 14: 94. https://doi.org/10.1038/s41419-023-05634-1.

[11] Wei B, Su Z, Yang H, Feng Y, Meng C, Liang Z. Inhibition of TRAF6 improves hyperlipidemic acute pancreatitis by alleviating pyroptosis in vitro and in vivo rat models. Biology Direct. 2023; 18: 23. https://doi.org/10.1186/s13062-023-00380-y.

[12] Wang X, Cai H, Chen Z, Zhang Y, Wu M, Xu X, *et al*. Baicalein alleviates pyroptosis and inflammation in hyperlipidemic pancreatitis by inhibiting NLRP3/Caspase-1 pathway through the miR-192-5p/TXNIP axis. International Immunopharmacology. 2021; 101: 108315. https://doi.org/10.1016/j.intimp.2021.108315.

[13] Liao Z, Zhang X, Song C, Lin W, Cheng Y, Xie Z, *et al*. ALV-J inhibits autophagy through the GADD45β/MEKK4/P38MAPK signaling pathway and mediates apoptosis following autophagy. Cell Death & Disease. 2020; 11: 684. https://doi.org/10.1038/s41419-020-02841-y.

[14] Mamontova V, Trifault B, Burger K. Nono induces Gadd45b to mediate DNA repair. Life Science Alliance. 2024; 7: e202302555. https://doi.org/10.26508/lsa.202302555.

[15] Shen XY, Shi SH, Li H, Wang CC, Zhang Y, Yu H, *et al*. The role of Gadd45b in neurologic and neuropsychiatric disorders: An overview. Frontiers in Molecular Neuroscience. 2022; 15: 1021207. https://doi.org/10.3389/fnmol.2022.1021207.

[16] Gupta SK, Gupta M, Hoffman B, Liebermann DA. Hematopoietic cells from gadd45a-deficient and gadd45b-deficient mice exhibit impaired stress responses to acute stimulation with cytokines, myeloablation and inflammation. Oncogene. 2006; 25: 5537–5546. https://doi.org/10.1038/sj.onc.1209555.

[17] Xue M, Sun H, Xu R, Wang Y, Guo J, Li X, *et al*. GADD45B Promotes Glucose-Induced Renal Tubular Epithelial-Mesenchymal Transition and Apoptosis *via* the p38 MAPK and JNK Signaling Pathways. Frontiers in Physiology. 2020; 11: 1074. https://doi.org/10.3389/fphys.2020.01074.

[18] Dong Y, Ma N, Fan L, Yuan L, Wu Q, Gong L, *et al*. GADD45β stabilized by direct interaction with HSP72 ameliorates insulin resistance and lipid accumulation. Pharmacological Research. 2021; 173: 105879. https://doi.org/10.1016/j.phrs.2021.105879.

[19] Pan Y, Li Y, Gao L, Tong Z, Ye B, Liu S, *et al*. Development of a novel model of hypertriglyceridemic acute pancreatitis in mice.

Scientific Reports. 2017; 7: 40799. https://doi.org/10.1038/srep40799.

[20] Yang C, Tian W, Ma S, Guo M, Lin X, Gao F, *et al*. AAV-Mediated ApoC2 Gene Therapy: Reversal of Severe Hypertriglyceridemia and Rescue of Neonatal Death in ApoC2-Deficient Hamsters. Molecular Therapy. Methods & Clinical Development. 2020; 18: 692–701. https://doi.org/10.1016/j.omtm.2020.07.011.

[21] Schmidt J, Rattner DW, Lewandrowski K, Compton CC, Mandavilli U, Knoefel WT, *et al*. A better model of acute pancreatitis for evaluating therapy. Annals of Surgery. 1992; 215: 44–56. https://doi.org/10.1097/00000658-199201000-00007.

[22] Feng P, Xu Y, Tong B, Tong X, Bian Y, Zhao S, *et al*. Saikosaponin a attenuates hyperlipidemic pancreatitis in rats via the PPAR-γ/NF-κB signaling pathway. Experimental and Therapeutic Medicine. 2020; 19: 1203–1212. https://doi.org/10.3892/etm.2019.8324.

[23] Ai Y, Meng Y, Yan B, Zhou Q, Wang X. The biochemical pathways of apoptotic, necroptotic, pyroptotic, and ferroptotic cell death. Molecular Cell. 2024; 84: 170–179. https://doi.org/10.1016/j.molcel.2023.11.040.

[24] Adiamah A, Psaltis E, Crook M, Lobo DN. A systematic review of the epidemiology, pathophysiology and current management of hyperlipidaemic pancreatitis. Clinical Nutrition (Edinburgh, Scotland). 2018; 37: 1810–1822. https://doi.org/10.1016/j.clnu.2017.09.028.

[25] Scherer J, Singh VP, Pitchumoni CS, Yadav D. Issues in hypertriglyceridemic pancreatitis: an update. Journal of Clinical Gastroenterology. 2014; 48: 195–203. https://doi.org/10.1097/01.mcg.0000436438.60145.5a.

[26] Patel K, Trivedi RN, Durgampudi C, Noel P, Cline RA, DeLany JP, *et al*. Lipolysis of visceral adipocyte triglyceride by pancreatic lipases converts mild acute pancreatitis to severe pancreatitis independent of necrosis and inflammation. The American Journal of Pathology. 2015; 185: 808–819. https://doi.org/10.1016/j.ajpath.2014.11.019.

[27] Xu T, Sheng L, Guo X, Ding Z. Free Fatty Acid Increases the Expression of NLRP3-Caspase1 in Adipose Tissue Macrophages in Obese Severe Acute Pancreatitis. Digestive Diseases and Sciences. 2022; 67: 2220–2231. https://doi.org/10.1007/s10620-021-07027-w.

[28] Meng N, Yang H, Chen J, Qin Y, Lei Y, Huang Z, *et al*. Honokiol reduces oxidative stress by activating the SIRT3-MnSOD2 pathway to alleviate hypertriglyceridemia-induced acute pancreatitis in rats. Nan Fang Yi Ke Da Xue Xue Bao = Journal of Southern Medical University. 2023; 43: 405–411. https://doi.org/10.12122/j.issn.1673-4254.2023.03.10.

[29] Vasudevan SO, Behl B, Rathinam VA. Pyroptosis-induced inflammation and tissue damage. Seminars in Immunology. 2023; 69: 101781. https://doi.org/10.1016/j.smim.2023.101781.

[30] Liu J, Zheng Y, Yang S, Zhang L, Liu B, Zhang J, *et al*. Targeting antioxidant factor Nrf2 by raffinose ameliorates lipid dysmetabolism-induced pyroptosis, inflammation and fibrosis in NAFLD. Phytomedicine: International Journal of Phytotherapy and Phytopharmacology. 2024; 130: 155756. https://doi.org/10.1016/j.phymed.2024.155756.

[31] Zheng X, Wan J, Tan G. The mechanisms of NLRP3 inflammasome/pyroptosis activation and their role in diabetic retinopathy. Frontiers in Immunology. 2023; 14: 1151185. https://doi.org/10.3389/fimmu.2023.1151185.

[32] Zeng Y, Liu X, Yi Q, Qiao G, Wang L, Chen L, *et al*. Free total rhubarb anthraquinones protect intestinal mucosal barrier of SAP rats via inhibiting the NLRP3/caspase-1/GSDMD pyroptotic pathway. Journal of Ethnopharmacology. 2024; 326: 117873. https://doi.org/10.1016/j.jep.2024.117873.

[33] de Vasconcelos NM, Van Opdenbosch N, Van Gorp H, Parthoens E, Lamkanfi M. Single-cell analysis of pyroptosis dynamics reveals conserved GSDMD-mediated subcellular events that precede plasma membrane rupture. Cell Death and Differentiation. 2019; 26: 146–161. https://doi.org/10.1038/s41418-018-0106-7.

[34] Chen Z, Wan X, Hou Q, Shi S, Wang L, Chen P, *et al*. GADD45B mediates podocyte injury in zebrafish by activating the ROS-GADD45B-p38 pathway. Cell Death & Disease. 2016; 7: e2068. https://doi.org/10.1038/cddis.2015.300.

[35] Li Z, Chi H, Zhu W, Yang G, Song J, Mo L, *et al*. Cadmium induces renal inflammation by activating the NLRP3 inflammasome through ROS/MAPK/NF-κB pathway in vitro and in vivo. Archives of Toxicology. 2021; 95: 3497–3513. https://doi.org/10.1007/s00204-021-03157-2.

[36] Zhen H, Hu Y, Liu X, Fan G, Zhao S. The protease caspase-1: Activation pathways and functions. Biochemical and Biophysical Research Communications. 2024; 717: 149978. https://doi.org/10.1016/j.bbrc.2024.149978.

[37] Zhan Y, Huang Q, Deng Z, Chen S, Yang R, Zhang J, *et al*. DNA hypomethylation-mediated upregulation of GADD45B facilitates airway inflammation and epithelial cell senescence in COPD. Journal of Advanced Research. 2025; 68: 201–214. https://doi.org/10.1016/j.jare.2024.02.005.

[38] Guo C, Li W, Liu Y, Tao X, Mahaman YAR, Wang J, *et al*. EPO Deficiency Upregulates GADD45b/p38 MAPK Axis, Mediating Schizophrenia-Related Synaptic and Cognitive Impairments. Advanced Science (Weinheim, Baden-Wurttemberg, Germany). 2024; 11: e2406979. https://doi.org/10.1002/advs.202406979.

[39] Wu S, Guo W, Chen L, Lin X, Tang M, Lin C, *et al*. Downregulation of Gadd45β alleviates osteoarthritis by repressing lipopolysaccharide-induced fibroblast-like synoviocyte inflammation, proliferation and migration. International Immunopharmacology. 2024; 126: 111202. https://doi.org/10.1016/j.intimp.2023.111202.

[40] Bai Y, Shen Y, Xu XY, Bai Y, Fang Y, Zhang M, *et al*. Growth arrest and DNA damage inducible 45-beta activates pro-inflammatory cytokines and phagocytosis in the grass carp (Ctenopharyngodon idella) after Aeromonas hydrophila infection. Developmental and Comparative Immunology. 2018; 87: 176–181. https://doi.org/10.1016/j.dci.2018.06.010.

[41] Lu B. The molecular mechanisms that control function and death of effector CD4+ T cells. Immunologic Research. 2006; 36: 275–282. https://doi.org/10.1385/IR:36:1:275.